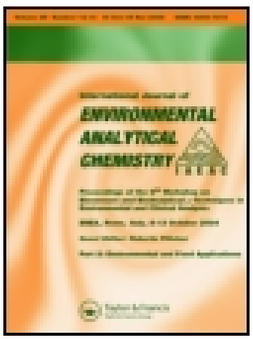

International Journal of Environmental Analytical Chemistry

ISSN: 0306-7319 (Print) 1029-0397 (Online) Journal homepage: https://www.tandfonline.com/loi/geac20

Determination of picric acid using micro CdS crystal-modified glassy carbon electrode

Y. Z. Song, X. J. Pang, J. Chen, Y. T. Lu, Jimin Xie & Yong Ye

To cite this article: Y. Z. Song, X. J. Pang, J. Chen, Y. T. Lu, Jimin Xie & Yong Ye (2019): Determination of picric acid using micro CdS crystal-modified glassy carbon electrode, International Journal of Environmental Analytical Chemistry, DOI: 10.1080/03067319.2019.1646257

To link to this article: https://doi.org/10.1080/03067319.2019.1646257

Published online: 24 Jul 2019.

INTERNATIONAL JOURNAL OF ENVIRONMENTAL ANALYTICAL CHEMISTRY
https://doi.org/10.1080/03067319.2019.1646257

Taylor & Francis
Taylor & Francis Group

ARTICLE

Determination of picric acid using micro CdS crystal-modified glassy carbon electrode

Y. Z. Song[a], X. J. Pang[a], J. Chen[a], Y. T. Lu[a], Jimin Xie[b] and Yong Ye[c]

[a]Jiangsu Province Key Laboratory for Chemistry of Low-Dimensional Materials, School of Chemistry & Chemical Engineering, Huaiyin Normal University, Huai An, People's Republic of China; [b]School of Chemistry & Chemical Engineering, Jiangsu University, Zhenjiang, People's Republic of China; [c]School of Chemistry, Hubei University, Wuhan, People's Republic of China

ABSTRACT

Picric acid is a dangerous environmental pollutant due to its high toxicity, and the detection of picric acid in the environment is of great significance. The Cd^{2+} on the surface of CdS crystals can enrich negative ionic compound to form a complex in water. Therefore, the micro CdS crystals have been synthesised using thioacetamide and cadmium sulfate by means of a simple and cheap hydrothermal method for the detection of picric acid and were characterised by means of X-ray diffractometer, scanning electron microscopy, energy-dispersive spectrometer and AC impedance technique. The electrochemical reduction of picric acid at micro CdS crystal-modified glassy carbon electrode was investigated, revealing that the micro CdS crystals could catalyze picric acid, and the reduction mechanism of picric acid on the surface of micro CdS crystals was also discussed. Based on the reduction of picric acid at the modified electrode, a simple method of detection for picric acid was proposed by applying voltammetry, and a linear regression equation was obtained as I (10^{-5}A) = 6160.53279 c (mol.L^{-1}) + 2.51034 (R = 0.9997) with a recoveries of 96.0–101.0% and relative standard deviations of 1.3–2.9% (n = 6), confirming very high sensitivity and selective detection of picric acid at the micro CdS crystal-modified glassy carbon electrode.

ARTICLE HISTORY
Received 5 April 2019
Accepted 3 June 2019

KEYWORDS
Picric acid; micro CdS crystals; modified electrode; electrochemical behaviour

1. Introduction

Picric acid, 2,4,6-trinitrophenol (TNP), is a phenol compound of trinitro-substituted group, which has strong acidity due to the electronic absorption of nitro groups. Long-term exposure to TNP causes headache, dizziness, nausea and vomiting, loss of appetite, diarrhoea, haemorrhagic nephritis, hepatitis, jaundice and damage of red blood cells. In addition, TNP is an active compound, and the friction, vibration and high temperature can cause explosion [1]. Therefore, many determination methods, such as spectrophotometric method [2], high-performance liquid chromatography [3], voltammetry [4], mass spectrometry [5] and Raman spectroscopy [6], have been applied for the detection of TNP.

CONTACT Y. Z. Song songyuanzhi@126.com

Voltammetry is a high-sensitivity and low-cost method. Moreover, the operation is very simple and fast. The modified electrodes have been attracting considerable attention in the determination of TNP due to their high active surface area. Many modified materials, such as graphene [7], carbon dots [8], cauliflower-shaped ZnO nanomaterials [9], gold nanoparticles [10], carbon nanotubes [11], graphene nanoribbons [12], mesoporous SiO_2 layers and poly(diallyldimethylammonium chloride) [13], poly[meso-tetrakis (2-thienyl) porphyrin] [14] and Prussian blue film [15], have been applied for the determination of TNP.

Cadmium sulfide has been extensively studied due to its excellent optical and electrical properties. Nano-sized or micro nanoscale cadmium sulfide is widely used in supercapacitor [16], photocatalysis [17,18], solar cell [19] and the sensor [20–22] because of its unique crystal structure. Hydrothermal synthesis of cadmium sulfide has the advantages of high yield, large-scale production, simple process, low cost, low pollution and mild reaction conditions. However, the shape and size of nanoparticles have a great influence on their physical and chemical properties and are controlled by not only the precursor but also the solvent, the reaction temperature, the reaction time, pH values of solution and the added surfactant. Thioacetamide is usually used as a precursor of sulfur in the synthesis of CdS. The nano CdS hollow microspheres [23], micro-size CdS spheres of hollow shape [24], CdS nanorods, urchin-like-shaped CdS [25] and its composites, such as $MoSe_2/MoS_2$/cCdS nanocomposites [26], g-C_3N_4/CdS/rGO [27] and CdS/g-C_3N_4/CuS composite [28], have been prepared using thioacetamide.

In this work, the micro CdS crystals were synthesised by hydrothermal method, and the electrochemical reduction of TNP at micro CdS crystal-modified glassy carbon electrode (GCE) was investigated. A simple method of detection for TNP was proposed.

2. Experimental

2.1. Regents

TNP, cadmium sulfate, thioacetamide, absolute ethyl alcohol and sodium dihydrogen phosphate were purchased from the National Research Center for CRM'S (Beijing, China). All other reagents were of analytical grade. Double-distilled water was used throughout; 0.1 M phosphate buffer solution was prepared by dissolving 0.1 mol NaCl and 0.1 mol Na_2HPO_4 in the double-distilled water of 1000 mL, and the desired pH values were adjusted with 1 mol.L^{-1} HCl or 1 mol.L^{-1} NaOH.

2.2. Instrument and characterisation

For all electrochemical experiments, a CHI660E Electrochemical Analyzer (CHI, USA) was employed. The electrochemical cells consisted of three electrodes: the micro CdS crystal-modified GCE was used as the working electrode and a platinum wire and a saturated calomel electrode (SCE) served as the counter electrode and the reference electrode, respectively. The micro CdS crystals were characterised by scanning electron microscope (QUANTA FEG 450, USA) equipped with an EDAX OCTANE PRO energy-dispersive spectrometer (EDS) (FEI, USA). X-ray diffraction (XRD) analysis was performed on the as-prepared products with a Switzerland ARLX'TRA X-ray diffractometer rotating

anode with Cu–K a radiation source (I = 0.1540562 nm). The electrochemical impedance spectroscopy (EIS) was measured at the open-circuit potential over the frequency range of 10^5 to 0.02 Hz with an AC amplitude of 5 mV.

2.3. Prepared modified electrode

The micro CdS crystals were prepared by the following methods: The thioacetamide of 0.06 mol and $CdSO_4.H_2O$ of 0.05 mol dissolved in the solution of water of 10 ml and absolute ethanol of 5 ml, and the mixture was sealed in a 30 ml polytetrafluoroethylene reaction jars. After sonicating for 30 min, the mixture was placed in an oven of 150℃ for 2 h, and then the cooled sample was washed with water for five times and absolute alcohol for four times, respectively, and dried in a vacuum dryer at 40℃ for 24 h.

Before preparation of the micro CdS crystal-modified GCE, a 3-mm-diameter disc GCE was polished with 0.05 μm alumina slurry on a polishing cloth, rinsed thoroughly with double-distilled water and then sonicated in ethanol and double-distilled water for 10 min, sequentially. The modifier suspension of 1 $mg.ml^{-1}$ CdS was prepared by dispersing the CdS crystals in 5.0 ml of N,N-dimethylformamide under sonication for 10 min. The micro CdS crystal-modified GCE was prepared by casting the CdS suspension of 5 μl on the GCE surface using a micropipette and left to dry at room temperature. Before the voltammetric measurements, the modified electrode was cycled between 0.75 and −2 V (scan rate 100 $mV.s^{-1}$) in 0.1 M phosphate buffer solution of pH 8.0 for several times until acquiring the reproducible responses. In order to avoid the dissolution of micro CdS crystals on the modified electrode, 0.1 $mol.L^{-1}$ phosphate buffer solution of pH 8.0 was used as supporting electrolyte in all voltammetric determinations.

3. Results and discussion

3.1. Morphology and grain diameter distribution of the micro CdS crystal

The morphology and grain diameter distribution of the micro CdS crystals are showed in Figure 1. From Figure 1, it could be seen that the smooth and regular particles were found in the as-prepared sample, and the particle sizes of CdS crystals were in the range of 0.26–1.02 um (average particle size of about 520 nm).

3.2. XRD and EDS spectrum of micro CdS crystal

Figures 2 and 3 show the XRD and EDS spectrum of micro CdS crystals, respectively. The pattern in Figure 3 matches quite well with the standard diffraction data of the CdS crystals (Pyrrhotite, JCPDS File No. 86–0389) and the previous reports [29]. In Figure 2, the peaks at 2θ values of 25.1°, 26.7°, 28.5°, 36.8°, 43.9°, 48.1°, 50.0°, 51.3°, 52.1°, 53.0°, 58.8°, 61.1°, 66.9°, 69.7°, 71.0°, 72.7°, 75.8° and 78.6° could be indexed to the (1 0 0), (0 0 2), (1 0 1), (1 0 2), (1 1 0), (1 0 3), (200), (1 1 2), (2 0 1), (004), (202), (104), (203), (210), (211), (114), (105) and (204) planes of CdS, respectively. The Cd, S and Au elements sprayed on the surface of the CdS are found in Figure 3, and they indicated that no other elements existed in the sample, and the atom ratio of S: Cd is 1.12.

3.3. EIS spectra of bare GCE and CdS-modified GCE

The EIS of bare GCE (a) and CdS-modified GCE (b) in 5.00×10^{-4} mol.L^{-1} TNP dissolved in the supporting electrolyte is shown in Figure 4. The contact resistances of bare GCE between the

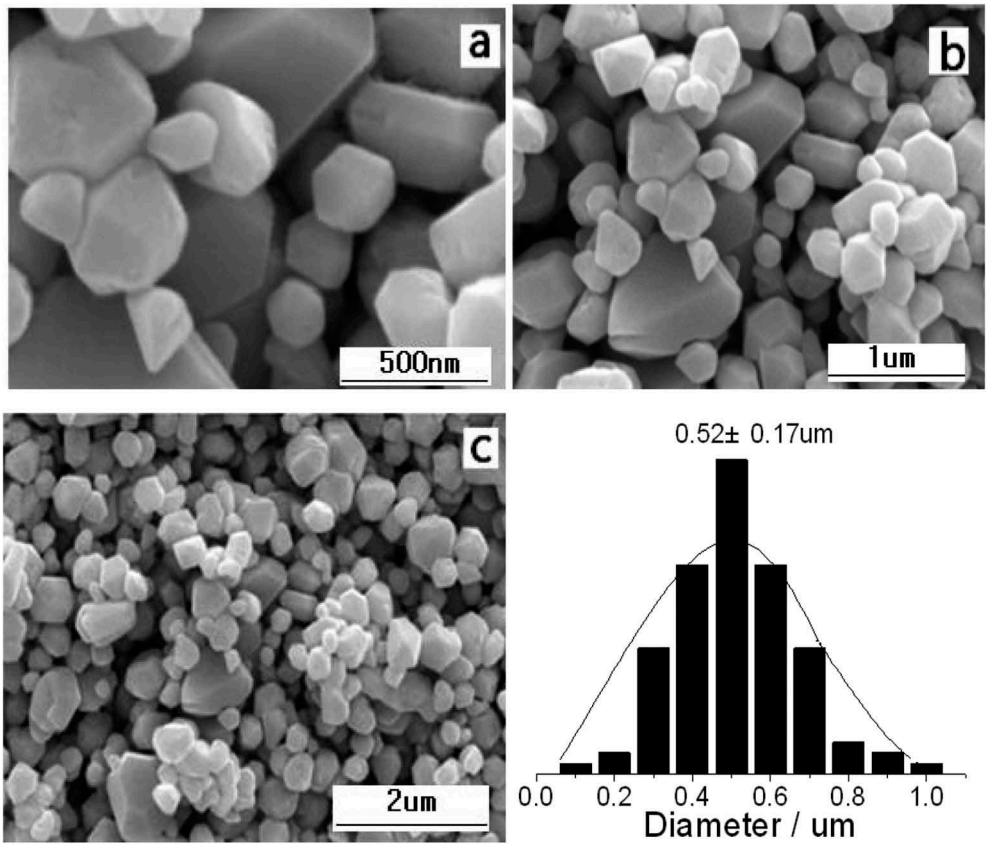

Figure 1. SEM images (a–c) and grain diameter distribution (d) of CdS.

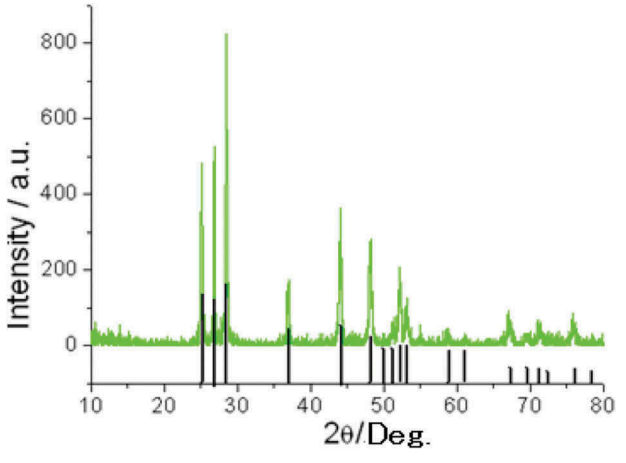

Figure 2. XRD spectrum of CdS.

solution and electrode were less than that of the CdS-modified GCE, while the charge transfer resistances (R_{ct}) of bare GCE were markedly more than that of the CdS-modified GCE, indicating that the CdS on the surface of GCE accelerates TNP charge transfer.

3.4. Electrochemical response of TNP on the CdS/GCE

The electrochemical response of TNP on the CdS/GCE in 0.1 M phosphate buffer solution of pH 8.0 is shown in Figure 5. From the cyclic voltammograms (CVs), a weak reduction

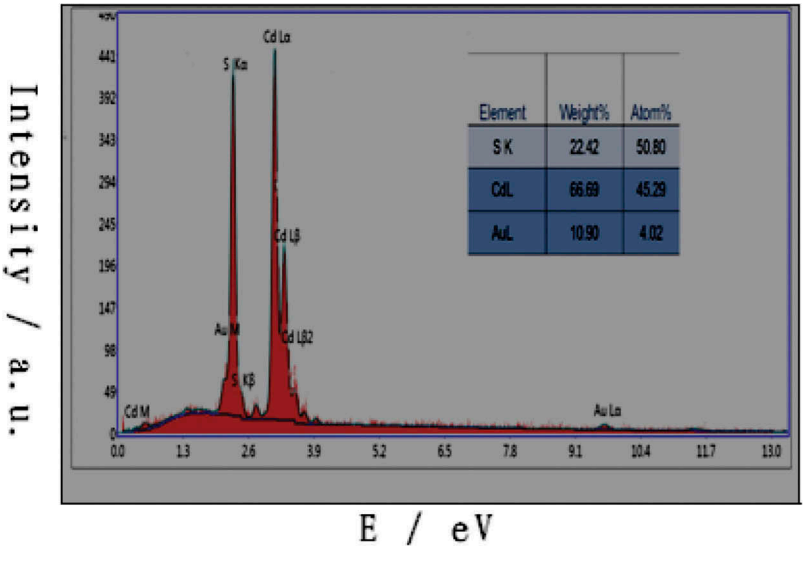

Figure 3. EDS spectrum of CdS.

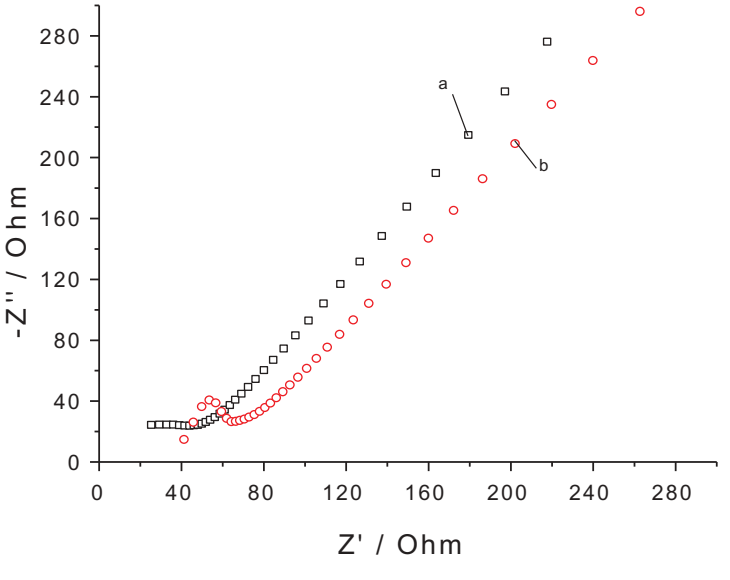

Figure 4. EIS of bare GCE (a) and micro CdS-modified GCE (b).

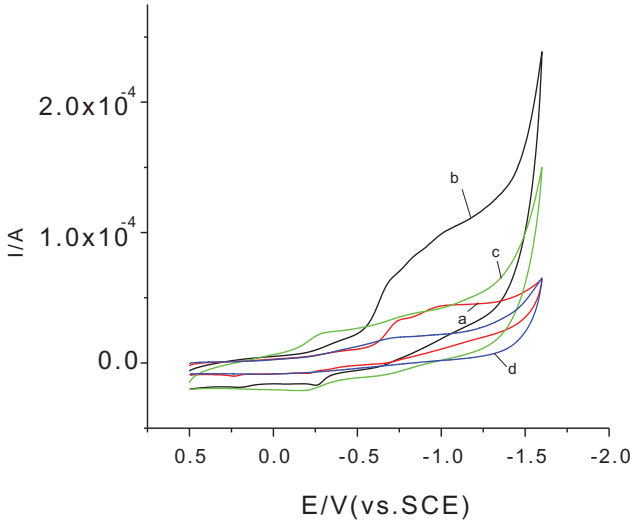

Figure 5. CVs of 5.00×10^{-4} mol.L^{-1} TNP on bare GCE (a) and CdS/GCE (b). CVs of CdS/GCE (c) and bare GCE (d) in 0.1 M phosphate buffer solution of pH 8.0. Scan rate: 100 mV.s^{-1}.

peak of oxygen at bare GCE and CdS-modified GCE was found, respectively. The broad reduction peak for TNP at bare GCE was also observed and is consistent with the reduction peak at about −0.6 to −0.8 V vs. SCE of TNP on the Bi, Cu, GC and Pt electrodes in a phosphate buffer solution of pH 7.4 [30]. Compared with the CVs of bare GCE, the peaks of TNP at CdS/GCE in Figure 5 shifted to positive direction, and the peak current observably increased, indicating that the CdS-modified electrode promoted the electrochemical reduction of TNP by considerably accelerating the rate of electron transfer.

The relationship between the reduction peak current and the concentration of TNP on the surface of CdS/GCE was examined by CVs in Figure 6(a) and amperometric i-t curve at −0.738 V (vs.SCE) in Figure 6(b), respectively. From Figure 6(a), the reduction peak currents were proportional to concentrations of TNP in the range of 1.0×10^{-3} to 9.0×10^{-3} mol.L^{-1} in 0.1 mol.L^{-1} supporting electrolyte, and a linear regression equation was obtained as I（10^{-5}A）(at −0.738 V) = 2.1353 + 6749 c（mol.L^{-1}）(R = 0.9965). Due to the absorption of products of reduced TNP ions on the surface of CdS, two regression equations in Figure 6(b) were obtained as I （10^{-5}A） = 1.7441 + 1891 c（mol.L^{-1}）(R = 0.9903) in the range of 1.0×10^{-4} to 1.90×10^{-3} mol.L^{-1} and I （10^{-5}A） = −1.17733 + 3522.9 c（mol.L^{-1}）(R = 0.9979) in the range of 1.9×10^{-4} to 4.5×10^{-3} mol.L^{-1}, respectively, and their respective detection limits calculated from the formula 3×(standard deviation of blank solution)/slope was 1.4 mmol.L^{-1} and 1.5 mmol.L^{-1}, which was close to the values of solid amalgam composite electrode [31]. Table 1 lists the detection limit, potential and electrodes used in the literature and in the proposed method for the electrochemical TNP analysis. Two oxidation peaks of higher concentration TNP were found, and their currents increased with the increase of TNP concentration, indicating that the reduction peaks were attributed to the reduction of TNP.

The influence of scan rate on the CV curves is shown in Figure 7, and the peak currents at −1.000 V (vs. SCE) increased with the increase of scan rate. An equation for this relationship was obtained as I (10^{-5}A) = 1.15779 + 0.66534 υ $^{1/2}$(mV. s^{-1}) (R = 0.9976; inset in Figure 7), indicating that the electrode process was controlled by the diffusion.

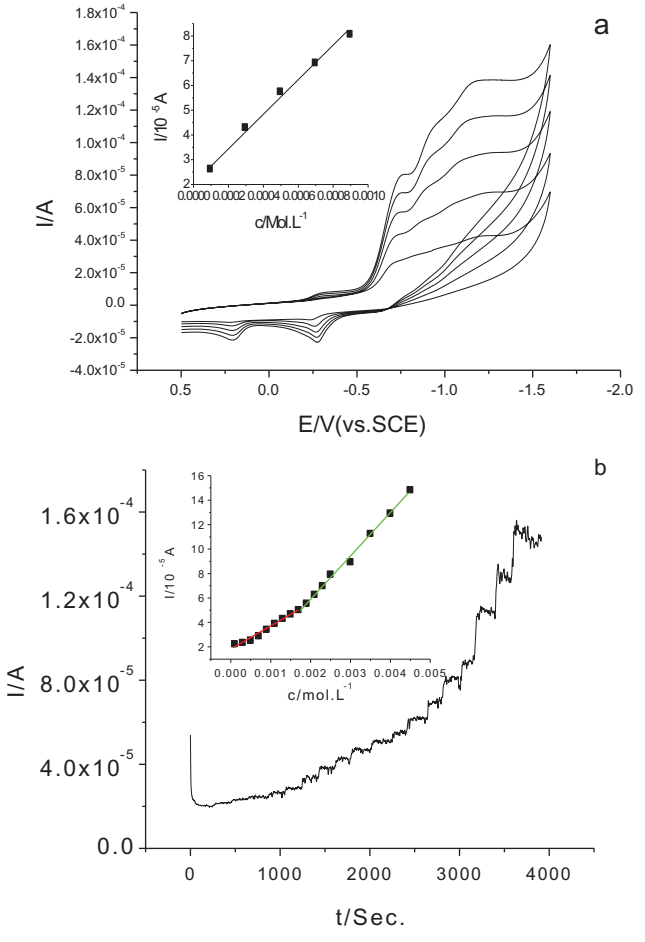

Figure 6. Relationship between the peak of CVs (a) and i-t curve at −0.738 V (vs. SCE) (b) current and concentration. Inset: plot of the peak current against the concentration. Scan rate: 100 mV.s^{-1}.

Table 1. Detection limit, potential and electrodes used in the literature and in the proposed method.

Reference	LD (mmol. L^{-1})	Linear range (mmol. L^{-1})	E (V)	Electrode
[30]	6×10^{-3}	$20–300 \times 10^{-3}$	−0.9 vs. Ag/AgCl (KCl sat.)	Copper electrode
[31]	1	–	−1.1 vs. Ag/AgCl (1 M KCl sat.)	Solid amalgam composite electrode
[32]	1.3×10^{-3}	$4.5–30 \times 10^{-3}$	−0.735 vs. SCE	Bismuth electrode
[33]	13×10^{-3}	$2.5 \times 10^{-2}–100$	Potentiometric sensor	$Cu/Hg/Hg_2(Pic)_2$/graphite
Proposed method	1.4–1.5	0.10–1.90	Amperometric i-t curve at −0.738 V vs. SCE	CdS/GCE

The influence of pH on the electrochemical behaviour of TNP was investigated at different pH values in the range of 5.0–10.0. Figure 8 shows the CVs of 5.00×10^{-4} mol. L^{-1} TNP on the modified electrode over the discussed pH ranges at the scan rate of 100 mV. s^{-1}. The peaks shifted to negative direction with the increase of pH values, and the

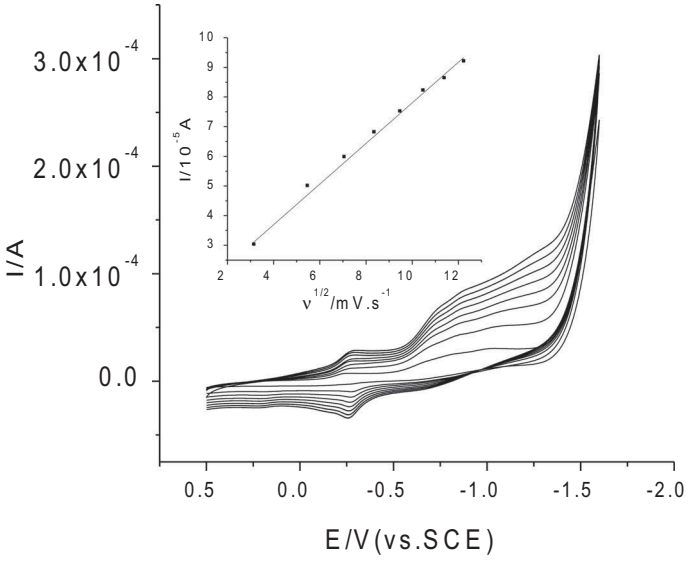

Figure 7. The influence of the scan rate on the CVs.

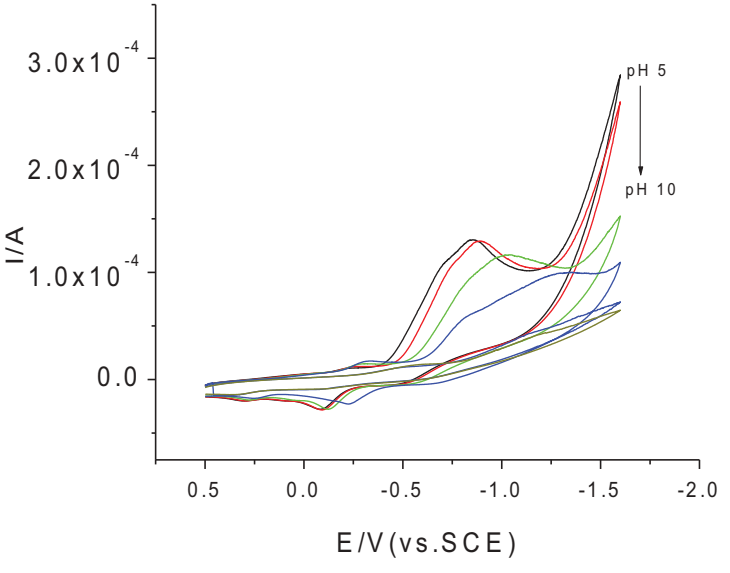

Figure 8. Infuence of pH on the shape of the cathodic peak of 5.00×10^{-4} mol.L^{-1} TNP. Scan rate: 100 mV.s^{-1}.

peak currents increased with the decrease of pH values, demonstrating that the hydrogen ions were involved in the reaction. When the pH values were less than 8, the peaks obviously change due to the ionisation of TNP.

It is generally admitted that nitro compounds are reduced as R–NO_2 + $4e^-$ + $4H^+$ = R–NHOH + $2H_2O$ [34]. The TNP in 0.1 mol.L^{-1} phosphate buffer of pH 8.0 ionised into

negative ions due to its high ionisation equilibrium constant (pKa = 0.38, 25℃ [35]). Compared with the CVs of TNP at the bare GCE in Figure 5, the reduction currents of TNP at the CdS-modified GCE in 0.1 mol.L^{-1} phosphate buffer solution of pH 8.0 were more than that of bare GCE, suggesting that the Cd^{2+} ions on the surface of micro CdS crystals adsorbed the TNP negative ions and formed complex, which could accelerate the electron transfer of TNP. The reduction mechanism of TNP is shown in Figure 9. The o-nitro group in the complex at low potential reduced as the route: first, TNP accepted two hydrogen ions and two electrons, lost a water molecule and then accepted two hydrogen ions and two electrons. Three reduction peaks of higher concentration of TNP were found in Figure 5; thus, another o-nitro group and the p-nitro group can reduce as above mentioned route.

3.5. Application

To assess the applicability of the proposed method, the modified GCE was applied for the determination of the content of TNP in artificial samples by applying voltammetry. Artificial samples were prepared by adding different concentrations of TNP into the lake water. The lake water of 5.00 ml was diluted to 10.0 ml with the supporting electrolyte of pH 8.0. The linear regression equation of the standard curve was obtained as I (10^{-5}A) = 6160.53279 c (mol.L^{-1}) + 2.51034 (R = 0.9997). The determination results using the standard addition method are shown in Table 2. The recoveries were in the range from 96.0% to 101.0% with relative standard deviation (RSD) of 1.3–2.9% (n = 6).

In order to study the interferences of some organic compounds and inorganic ions on the detection of TNP, 100-fold of Al^{3+}, Zn^{2+}, K^{+}, Na^{+}, Ca^{2+}, Mg^{2+}, Cu^{2+}, Ba^{2+}, Ca^{2+} and K^{+}, 100-fold of Br^{-}, Cl^{-}, NO_3^{-}, Ac- and SO_4^{2-} and fivefold of para-hydroxybenzoic acid, phenol, methylbenzene, resorcinol, salicylic acid, catechol, p-aminophenol, oxalic acid, glucose, fructose and malic acid in 1×10^{-4} mol.L^{-1} TNP did not interfere with the determination (signal change below 5%).

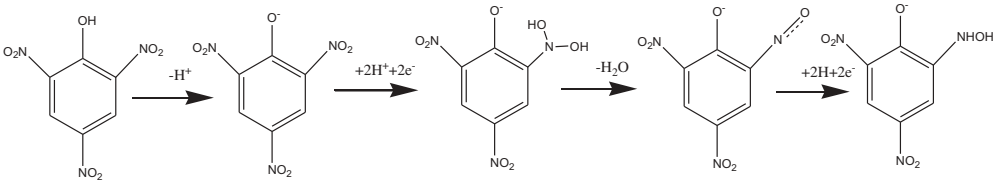

Figure 9. Mechanism of the electrochemical reduction of TNP.

Table 2. Recovery and RSD% of determination of TNP in water.

Sample	1	2	3	4
Conc. (10^{-4} mol.L^{-1})	1.00	3.00	5.00	7.00
Added (10^{-4} mol.L^{-1})	3.00	5.00	3.00	5.00
Found (10^{-4} mol.L^{-1})	3.96	7.90	8.03	11.80
RSD (% n = 6)	1.30	2.30	2.50	2.90
Recovery (%)	98.7	98.0	101.0	96.0

4. Conclusions

In the present work, the micro CdS crystals were prepared using hydrothermal method, and the electrochemical reduction of TNP at micro CdS crystal-modified GCE was investigated. The results indicate that the CdS has a certain catalytic effect on TNP, and the reduction mechanism and the application of TNP were also discussed.

Disclosure statement

No potential conflict of interest was reported by the authors.

Funding

This research was supported by the Opened Foundation of Jiangsu Province Key Laboratory for Chemistry of Low-Dimensional Materials (Grant No. JSKC17009).

References

[1] R. Hasegawa, M. Hirata-Koizumi, M. Dourson, A. Parker and M. Ema, Regul. Toxicol. Pharm. **47**, 296 (2007). doi:10.1016/j.yrtph.2006.10.003.
[2] M.E. Mohamed, E.Y.Z. Frag, A.A. Hathoot and E.A. Spectrochim, Acta. Part A **189**, 357 (2018). doi:10.1016/j.saa.2017.08.027.
[3] D. Norton, B. Crow, M. Bishop, K. Kovalcik, J. George and J.A. Bralley, J. Chromatogr. B **850**, 190 (2007). doi:10.1016/j.jchromb.2006.11.020.
[4] A. Kumar, A. Pandith and H.-S. Kim, Sens. Actuator B-Chem. **231**, 293 (2016). doi:10.1016/j.snb.2016.03.033.
[5] K. Hakansson, R.V. Coorey, R. Zubarev, V.L. Talrose and P. Hakansson, J. Mass. Spectrom. **35**, 337 (2000). doi:10.1002/1096-9888(200011)35:11<1335::AID-JMS70>3.0.CO;2-0.
[6] J.M. Sylvia, J.A. Janni, J.D. Klein and K.M. Spencer, Anal. Chem. **72**, 5834 (2000). doi:10.1021/ac0006573.
[7] J. Huang, L. Wang, C. Shi, Y. Dai, C. Gu and J. Liu, Sensor. Actuat. B **190**, 567 (2014). doi:10.1016/j.snb.2014.02.050.
[8] Z.F. Yu, Y. Zhang, N. Li, G.L. Shi, T. Liu, N.B. Li and H.Q. Luo, Sensor. Actuat. B **240**, 949 (2017). doi:10.1016/j.snb.2016.09.063.
[9] A.A. Ibrahim, R. Kumard, A. Umar, S.H. Kim, A. Bumajdade, Z.A. Ansarif and S. Baskoutasc, Electrochim. Acta. **222**, 463 (2016). doi:10.1016/j.electacta.2016.10.199.
[10] D. Nie, D. Jiang, D. Zhang, Y. Liang, Y. Xue, T. Zhou, L. Jin and G. Shi, Sensor. Actuat. B **156**, 43 (2011). doi:10.1016/j.snb.2011.03.071.
[11] H.L. Poh and M. Pumera, Chem. Asian J. **7**, 412 (2012). doi:10.1002/asia.201100681.
[12] M.S. Goh and M. Pumera, Anal. Bioanal. Chem. **399**, 127 (2011). doi:10.1007/s00216-010-3679-7.
[13] G. Shi, Y. Qu, Y. Zhai, Y. Liu, Z. Sun, J. Yang and L. Jin, Electrochem. Commun. **9**, 1719 (2007). doi:10.1016/j.elecom.2007.03.019.
[14] W. Chen, Y. Wang, C. Brueckner, C.M. Li and Y. Lei, Sensor. Actuat. B **147**, 191 (2010). doi:10.1016/j.snb.2010.03.046.
[15] D. Lu, A. Cagan, R.A.A. Munoz, T. Tangkuaram and J. Wang, Analyst **131**, 1279 (2006). doi:10.1039/b602546c.
[16] D.S. Patil, S.A. Pawar and J.C. Shin, Chem. Eng. J. **335**, 693 (2018). doi:10.1016/j.cej.2017.11.007.
[17] N. Zhu, J. Tang, C. Tang, P. Duan, L. Yao, Y. Wu and D.D. Dionysiou, Chem. Eng. J. **353**, 237 (2018). doi:10.1016/j.cej.2018.07.121.

[18] M. Shakir, M. Faraz, M.S. Khan and S. Ibrahim Al-Resayes, C. R. Chimie **18**, 966 (2015). doi:10.1016/j.crci.2015.07.009.
[19] E.N. Jayaweera, G.R.A. Kumar, C. Kumarage, S.K. Ranasinghe, R.M.G. Rajapakse, H.M. N. Bandar, O.A. Ileperuma and B.S. Dassanayake, J. Photoch. Photobiolo. A **364**, 109 (2018). doi:10.1016/j.jphotochem.2018.05.029.
[20] L. Ding, Y. Ruan, T. Li, J. Huang, S.C. Warren-Smith, H. Ebendorff-Heidepriem and T.M. Monro, Sensor. Actuat. B **273**, 9 (2018). doi:10.1016/j.snb.2018.06.012.
[21] M. Faraz, A. Abbasi, F.K. Naqvi, N. Khare, R. Prasad, I. Barman and R. Pandey, Sensor. Actuat. B **269**, 195 (2018). doi:10.1016/j.snb.2018.04.110.
[22] I. Barman and R. Pandey, Sensor. Actuat. B **269**, 195 (2018). doi:10.1016/j.snb.2018.04.110.
[23] M. Faraz, M. Shakir and N. Khare, New J. Chem. **41**, 5784 (2017). doi:10.1039/C7NJ01132F.
[24] S. Rengaraj, A. Ferancova, S.H. Jee, S. Venkataraj, Y. Kim, J. Labuda and M. Sillanpaeae, Electrochim. Acta. **56**, 501 (2010). doi:10.1016/j.electacta.2010.09.019.
[25] K.-H. Choi, W.-S. Chae, J.-S. Jung and Y.-R. Kim, B. Kor. Chem. Soc. **30**, 1118 (2009). doi:10.5012/bkcs.2009.30.12.3073.
[26] J. Yu, Y. Yu, P. Zhou, W. Xiao and B. Cheng, Appl. Catal. B **156–157**, 184 (2014). doi:10.1016/j.apcatb.2014.03.013.
[27] D.P. Kumar, E.H. Kim, H. Park, S.Y. Chun, M. Gopannagari, P. Bhavani, D.A. Reddy, J.K. Song and T.K. Kim, ACS App. Mater. Interf. **10**, 26153 (2018). doi:10.1021/acsami.8b02093.
[28] S. Tonda, S. Kumar, Y. Gawli, M. Bhardwaj and S. Ogale, Int. J. Hydrogen. Energy **42**, 5971 (2017). doi:10.1016/j.ijhydene.2016.11.065.
[29] F. Cheng, H. Yin and Q. Xiang, Appl. Surf. Sci. **391**, 432 (2017). doi:10.1016/j.apsusc.2016.06.169.
[30] X. Ma, X. Zhang, J. Gong, N. Wang, B. Fan and L. Qu, Cryst.Eng.Comm **14**, 246 (2012). doi:10.1039/C1CE05968H.
[31] J.R.C. Junqueira, W.R. de Araujo, M.O. Salles and T.R.L.C. Paixậon, Talanta. **104**, 162 (2013). doi:10.1016/j.talanta.2012.11.036.
[32] V. Vyskocil, T. Navratil, A. Danhel, J. Dedik, Z. Krejcova, L. Skvorova, J. Tvrdikova and J. Barek, Electroanalysis **23**, 129 (2011). doi:10.1002/elan.201000428.
[33] O. El Tall, D. Beh, N. Jaffrezic-Renault and O. Vittori, Int. J. Environ. Anal. Chem. **90**, 40 (2010). doi:10.1080/03067310902871265.
[34] M. Moghimi, M. Arvand, R. Javandel and M.A. Zanjanchi, Sensor. Actuat. B **107**, 296 (2005). doi:10.1016/j.snb.2004.10.015.
[35] R.S. Nicholson, J.M. Wilson and M.L. Olmstead, Anal. Chem. **38**, 542 (1966). doi:10.1021/ac60236a005.
[36] *CRC Handbook of Chemistry and Physics*, 82 ed. (2001～2002).